DESIGN CONCEPT ON REDUCTION OF HEATING AND AIR POLLUTION CONCENTRATIONS IN URBAN AREAS

Tetsuji Yamada*
Yamada Science & Art Corporation

Abstract

We determined through numerical simulations the cause for the surface temperature rise was the reduction of wind speeds by buildings. We proposed to raise building bases away from the ground so that buildings would not block air flows in the surface layer. If the building base was raised by 10 m above the ground, the ground temperature in the building areas decreased by 10 °C. When the building base was raised by 20 m or more, the ground temperatures were almost identical to those without buildings.

1. INTRODUCTION

We added CFD capabilities to a three-dimensional atmospheric model HOTMAC (Yamada and Bunker, 1988). The new model is referred to as A2Cflow where "A2C" stands for "Atmosphere to CFD." In this way, A2Cflow can simulate airflows from building to terrain scales in a seamless manner by nesting computational domains. In addition, the model physics become identical for the CFD and atmospheric components since the governing equations are same in a single model.

Affiliated with the A2Cflow is a three-dimensional transport and diffusion code "A2Ct&d" where "t&d" stands for transport and diffusion. A2Ct&d is based on a Lagrangian random walk theory (Yamada and Bunker, 1988). A2Cflow provides three-dimensional mean and turbulence distributions needed for A2Ct&d simulations.

2. MODELS

The governing equations for mean wind, temperature, mixing ratio of water vapor, and turbulence were similar to those used by Yamada and Bunker (1988). Turbulence equations were based on the Level 2.5 Mellor-Yamada second-moment turbulence-closure model (Mellor and Yamada, 1974, 1982). Five primitive equations were solved for ensemble averaged variables: three wind components, potential temperature, and mixing ratio of water vapor. In addition, two primitive equations were solved for turbulence: one for turbulence kinetic energy and the other for a turbulence length scale (Yamada, 1983).

The hydrostatic equilibrium is a good approximation in the atmosphere. On the other hand, air flows around buildings are not in the hydrostatic equilibrium because the pressure variations are generated by changes in wind speeds, and the resulted pressure gradients subsequently affect wind distributions.

We adopted the HSMAC (Highly Simplified Marker and Cell) method (Hirt and Cox, 1972) for non-hydrostatic pressure computation because the method is simple yet efficient. The method is equivalent to solving a Poisson equation, which is commonly used in non-hydrostatic atmospheric models.

Boundary conditions for the ensemble and turbulence variables were discussed in detail in Yamada and Bunker (1988). The temperature in the soil layer was obtained by numerically integrating a heat conduction equation. Appropriate boundary conditions for the soil temperature equation were the heat energy balance at the ground and specification of the soil temperature at a certain distance below the surface, where temperature was constant during the integration period. The surface heat energy balance was composed of solar radiation, long-wave radiation, sensible heat, latent heat, and soil heat fluxes.

Lateral boundary values for all predicted variables were obtained by integrating the corresponding governing equations, except that variations in the horizontal directions were all neglected. The upper level boundary values were specified and these values were incorporated into the governing equations through four-dimensional data assimilation or a "nudging" method (Kao and Yamada, 1988).

Initial and boundary conditions may be provided by other mesoscale models such as WRF/MM5, NCEP, and Japanese GPV.

Temperatures of building walls and roofs were computed by solving a one-dimensional heat conduction equation in the direction perpendicular to the walls and roofs. The boundary conditions were a heat balance equation at the outer sides of walls and roofs and room temperatures specified at the inner sides of the walls.

* 13 Heiwa, Santa Fe, NM 87506, U.S.A.

3. A2C CAPABILITIES

The A2C modeling system has been applied to wind tunnel to building to complex terrain scales. The following sections demonstrate some of the modeling capabilities.

3.1. Wind Tunnel Model Simulation

We simulated wind tunnel experiments reported in Tominaga et al. (2008). A simulation was conducted in a computational domain of 176 cm x 50 cm x 90 cm (vertical) with horizontal grid spacing of 1 cm.

The vertical grid spacing was 2 cm for the first 30 cm from the ground and increased gradually to the top of computational domain.

A model building of 8 cm (W) x 8 cm (D) x 16 cm (H) was placed along the centerline of the computational domain (2:1:1 block). Inflow boundary values of winds and TKE were specified by the measurements.

Figure 1 shows wind direction (arrows) and wind speed (color) distributions in a vertical cross section along the centerline of the computational domain.

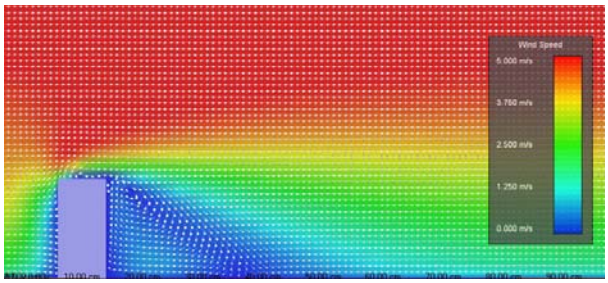

Fig. 1: The modeled wind distributions in a vertical cross section along the centerline of the computational domain

3.2. Thermal Effect of Building Wall Heating

We investigated thermal effect of buildings on the air flows and transport and diffusion of airborne materials around buildings.

The computational domain was 200 m x 200 m in the horizontal direction and 500 m in the vertical direction. Horizontal grid spacing was 4 m and the vertical grid spacing was 4 m for the first 15 levels and increased spacing gradually with height. There were 31 levels in the vertical direction.

Two buildings were placed along the centerline of the computational domain. The size of each building was 32 m x 32 m in the base and 30 m in height. Initial winds were westerly and 5 m/s throughout the computational domain. Boundary conditions for winds were 5 m/s at the inflow boundary and in the layers higher than 200 m from the ground. Those boundary conditions were maintained by using a nudging method.

Diurnal variations of building wall temperatures were obtained by solving a one-dimensional heat conduction equation in the direction perpendicular to the wall surfaces. The boundary conditions were the heat energy balance at the outer surfaces and constant temperature (25 $^{\circ}$C) specified at the inner surfaces.

Fig. 2 shows the modeled wind distributions at 2 p.m. in a vertical cross section along the centerline of the computational domain. The temperature on the wall facing west was approximately 40 $^{\circ}$C, which was significantly higher than the temperature on the wall facing east (approximately 20 $^{\circ}$C).

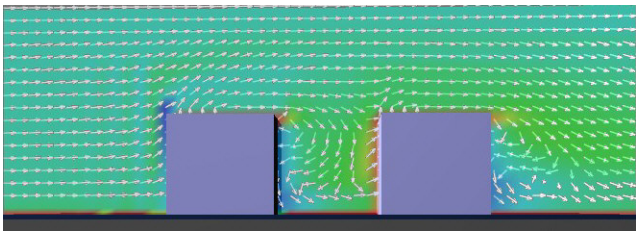

Fig. 2: The modeled wind distributions in a vertical cross section along the centerline of the computational domain at 2 p.m. Arrows indicate wind directions and colors indicate temperatures: red for 40 ^{o}C and green for 25 ^{o}C.

Under the neutral density stratification, recirculation flows were normally observed between the two buildings. Recirculation flows, however, disappeared when walls were heated or cooled as in the present case. There were upward motions along the warmer walls and downward motions along the cooler walls.

It is obvious from the simulations that air flows around buildings were quite different whether building wall temperatures were higher or lower than the air temperatures.

3.3. Building Exterior and Interior Airflows

We simulated both exterior and interior airflows of buildings. Two buildings were placed in a computational domain of 200 m x 200 m x 500 m (vertical). Horizontal grid spacing was 4 m and the vertical grid spacing was 4 m for the first 15 levels and increased spacing gradually with height. There were 31 levels in the vertical direction.

Several windows or doors were placed in the building walls so that air could circulate between the exterior and interior of buildings.

Fig. 3 shows modeled particle trajectories. Particles were released at a location inside of upper building and at an upstream side of the entrance of the lower building. Wind direction in the free atmosphere was from left to right (westerly) and wind speed was 5 m/s.

Building walls and roofs were made semi-transparent graphically so that trajectories inside building became visible. The walls and roofs were solid in the simulation.

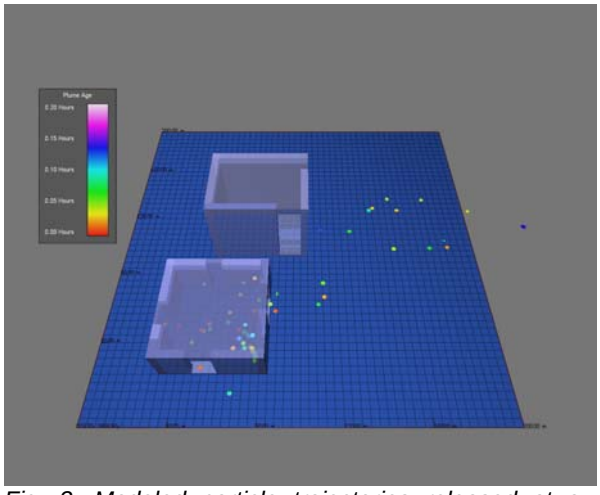

Fig. 3: Modeled particle trajectories released at a location inside of the upper building and at an upstream side of the entrance of the lower building

3.4. Urban Heat Island Mitigations

Simulations were performed to investigate the effects of the heating/cooling of building roofs/walls and blocking airflows by buildings on urban heat island (Control run). A second simulation was conducted by keeping the building temperatures at a constant value (25 °C) throughout the diurnal period (Constant building temperature run). A third simulation was performed where building bases were raised from the ground (Building base raised run).

3.4.1. Control run

We simulated diurnal variations of air flows around a cluster of buildings, which were bound by the ocean and hills (Fig. 4). Large cities are often located in a coastal area or near complex terrain.

Two inner domains were nested in a large domain (Fig. 5). The first domain was 6560 m x 8960 m with horizontal grid spacing of 160 m. The second domain was 1280 m x 1440 m with horizontal grid spacing of 40 m. The third domain was 360 m x 400 m with horizontal grid spacing of 10 m.

Domain 1 includes topographic features such as the ocean, coastal area, plains, and hills. Domain 2 is a transition area between Domain 1 and Domain 3. Buildings were located in Domain 3.

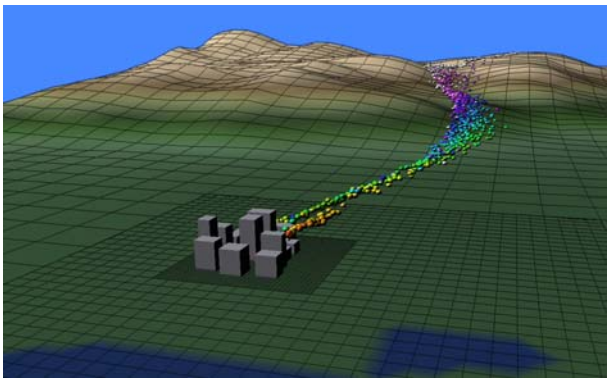

Fig. 4: Three dimensional image of the computational domain.

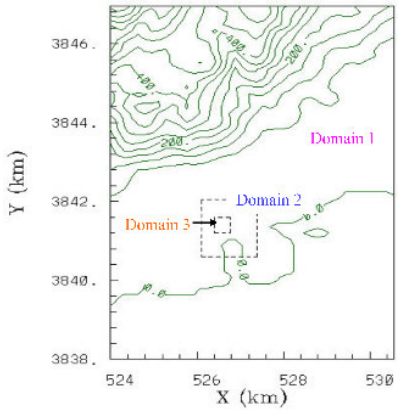

Fig.5: Computational domains: Domain 1 is the outer domain. Solid contour lines indicate ground elevations. Numerical numbers are altitudes in meters. Dashed lines indicate the boundaries of nested domains: Domain 2 and Domain 3.

The simulation area was around Kobe, Japan. Kobe is surrounded by the ocean in the south and Rokko Mountain in the north so that the sea and land breezed frequently occurred. The elevation data was extracted from the digital elevation data provided by the Japan Map Center.

Hypothetical buildings (13) were placed in Domain 3 whose heights varied from 30 m to 100 m. Thermal properties of the buildings were identical for all buildings and assumed to be the same as those for concrete.

Simulations initiated at 8 a.m., July 20 (Day 200) and continued for 48 hours. Initial wind directions were

westerly and wind speeds in the upper levels were 3 m/s. Initial temperatures at mean sea level was 25^{o} C. Potential temperature gradients in the vertical direction were 0.001 K/m for the first 1000 m above the ground and 0.003 K/m in the levels greater than 1000 m above the ground. The top of computational domain was 2000 m above the highest ground elevation (789 m for the present study).

Figure 6 shows wind and temperature distributions in Domain 1 at 2 m above the ground at 9:20 Day 200. Sea breezes in the coastal area and upslope flows over the Rokko Mountain were evident. Winds over the ocean and in the plain between the ocean and mountain remained westerly.

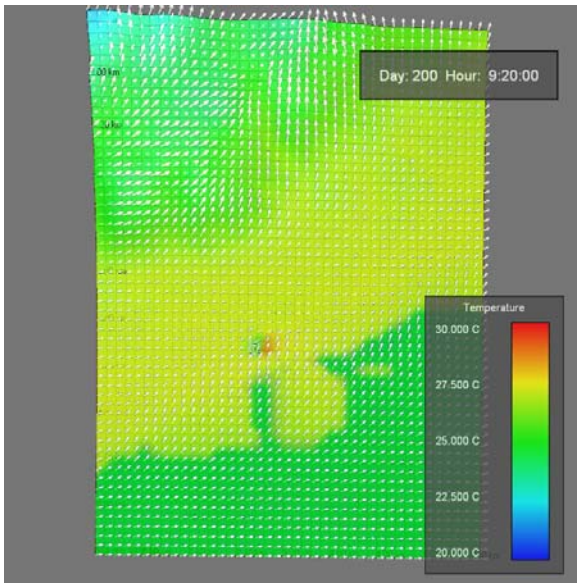

Fig. 6: Wind and temperature distributions in Domain 1 at 2 m above the ground at 9:20, July 20 (Day 200).

Figure 7 shows the corresponding distributions in Domain 2. Sea breeze penetration was blocked by building clusters.

Figure 8 shows the modeled temperature distributions along a vertical section at 13:00, Day 201. Note the temperature heat dome over the building cluster.

Figure 9 shows the ground temperature distributions at 12:00, Day 200. Ground temperature in the building cluster was much higher than those in the surrounding area. The main reason for the higher temperature was the reduction of wind speed (Fig. 10).

3.4.2. Constant building temperature run

We conducted simulations where building temperature were assumed to be constant (25 ^{o}C) throughout the simulation period. Other simulation conditions were identical to those for the control run.

Figure 11 shows wind and temperature distributions in Domain 2 at 2 m above the ground at 9:20, July 20 (Day 200). As expected there was no temperature hot spot in the eastern side of the building cluster compared with the counterpart of the control run (Fig. 7). Consequently wind directions in the temperature hot spot were also different.

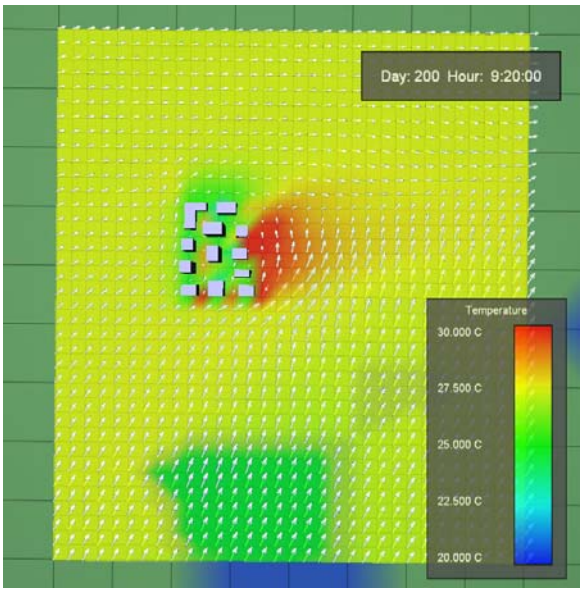

Fig. 7: *Wind and temperature distributions in Domain 2 at 2 m above the ground at 9:20, July 20 (Day 200).*

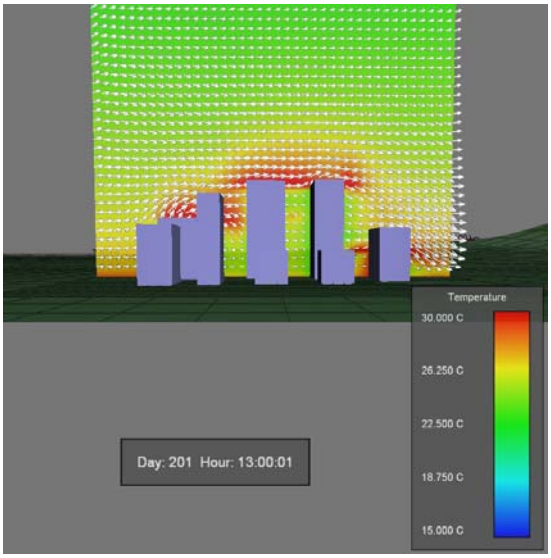

Fig. 8: Temperature distributions in a vertical cross section in the north-south direction at 13:00, Day 201.

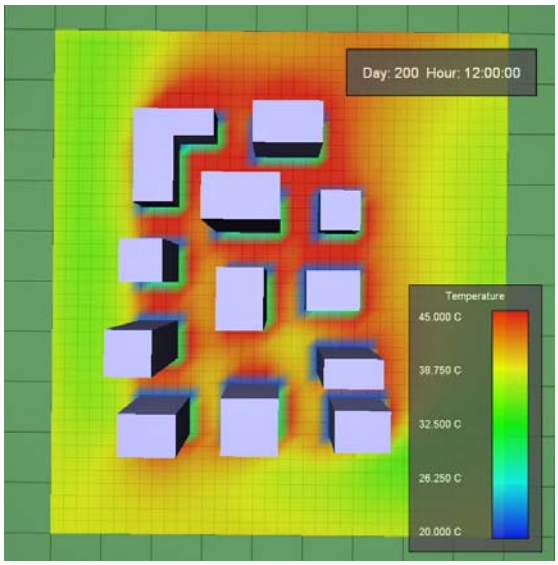

Fig. 9: The modeled surface temperature distributions at 12:00, Day 200.

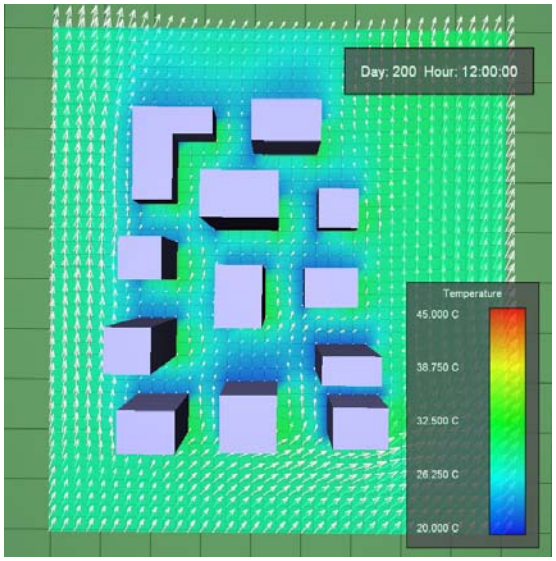

Fig. 10: The modeled wind distributions at 2 m above the ground at 12:00, Day 200.

Figure 12 shows the modeled temperature distributions along a vertical section in the north-south direction at 12:00, Day 200. As expected there was no heat dome over the buildings which was evident in the control run (Fig. 8).

The modeled ground temperature distributions (not shown) at 12:00, Day 200 were almost identical to those in the control run (Fig. 9). Although temperature distributions in the layers above the ground were significantly different, ground temperature remained essentially the same from the control run.

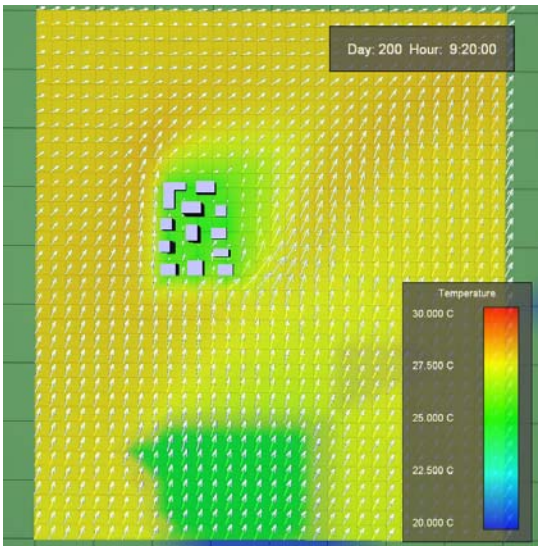

Fig. 11: Wind and temperature distributions in Domain 2 at 2 m above the ground at 9:20, July 20 (Day 200)

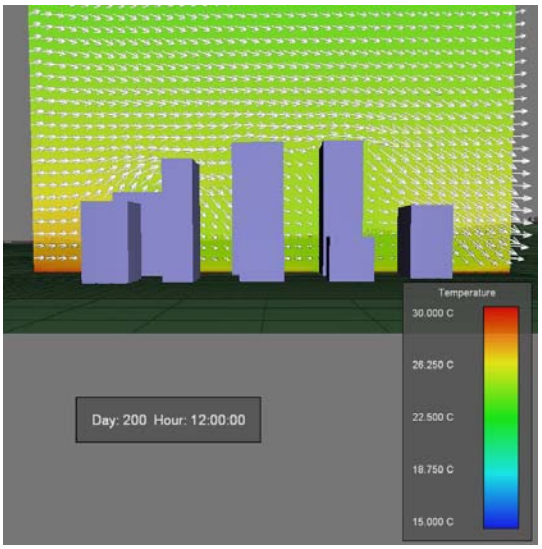

Fig. 12: Temperature distributions in a vertical cross section in the north-south direction at 12:00, Day 200.

3.4.3. Building base raised run

We conducted simulations where building bases were raised away from the ground so that building would not block the air flows in the surface layer (Fig. 13).

When the building base was raised by 10 m above the ground, then the ground temperatures in the building areas decreased by 10 °C from those for the control run (building base was at the ground). When building base was raised by 20 m or more, the ground temperatures were almost identical to those without buildings as shown in Fig. 14.

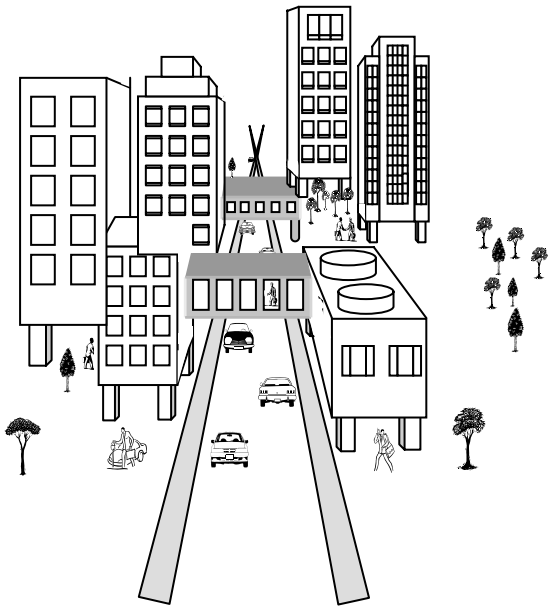

Fig. 13: Perspective view of buildings raised from the ground.

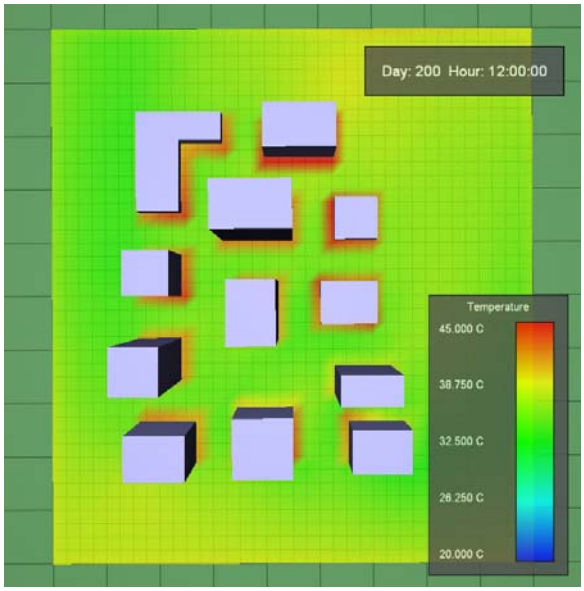

Fig. 14: The modeled surface temperature distributions at 12:00, Day 200.

Figure 15 shows wind distributions at 2 m above the ground. Wind distribution was much more uniform and wind speeds were significantly higher than those in Fig. 10.

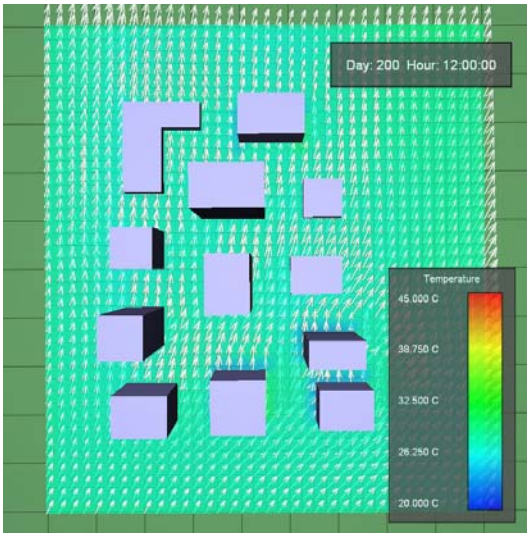

Fig. 15: The modeled wind distributions at 2 m above the ground at 12:00, Day 200.

4. SUMMARY

A three-dimensional atmospheric prediction model, A2Cflow, was improved: airflows not only in complex terrain, but also exterior and interior of buildings and in a wind tunnel were simulated.

We adopted HSMAC method for the non-hydrostatic pressure computation because it is simple yet efficient. The method is equivalent to solving a Poisson equation, which is commonly used in non-hydrostatic atmospheric models.

Airflows around a model building in a wind tunnel were simulated with horizontal grid spacing of 1 cm. Separation and reattachment of air flows at the leading edge and behind buildings were in good agreement of wind tunnel data.

Simulations were conducted to illustrate the thermal effects of building walls on the air flows around two (2) buildings. Building wall temperatures were computed by solving a one-dimensional heat conduction equation in a direction perpendicular to walls. Boundary conditions were a heat energy balance at the outer surfaces of buildings and temperatures specified at the inner surfaces.

When building walls were heated and cooled, air flows around two buildings became quite different from those without wall heating. Recirculation and

reattachment around buildings no longer existed. In general upward motions were simulated along warm walls and downward motions were simulated along cold walls.

Airflows exterior and interior of buildings were also investigated. Building interior flows were influenced by the locations of opening (windows and doors) and exterior flows. Exterior flows, on the other hand, were functions of local circulations resulted from topographic variations.

We simulated diurnal variations of air flows around a cluster of buildings, which were bound by the ocean and hills. Large cities are often located in a coastal area or near complex terrain. Prediction of transport and diffusion of air pollutants and toxic materials is of considerable interest to the safety of the people living in urban areas.

There were significant interactions between air flows generated by topographic variations and a cluster of buildings. Sea breeze fronts were blocked by buildings. Winds were calm in the courtyards. Winds diverged in the upstream side and converged in the downstream side of the building cluster.

Wind speeds and wind directions around buildings changed as the winds in the outer domains encountered diurnal variations. Domain 3 alone could not reproduce diurnal variations of winds because it didn't include topographic features responsible for mesoscale circulations such as sea/land breezes and mountain/valley flows.

On the other hand, Domain 1 alone could not depict the effects of buildings because the horizontal grid spacing (160 m) was too coarse to resolve buildings. Air flows around buildings were successfully simulated in Domain 3 and modified air flows in Domain 3 were transferred back to Domain 2 and Domain 1 through two-way nesting algorithm.

A few atmospheric models have both mesoscale and CFD scale modeling capabilities. However, we are not aware of any report that a single model was used to simulate interactions between mesoscale and CFD scale circulations.

Numerical simulations were conducted to study reduction of heat island effects when building wall temperatures were kept constant. As expected heat domes over buildings disappeared. However, ground temperature remained the same in the urban area where wind speeds were small.

We determined through our numerical simulations the cause for the surface temperature rise was the reduction of wind speeds by buildings. The surface temperature was determined from the heat energy balance at the ground. The balance was strongly affected by wind speed in the surface layer. The lower the wind speed, the higher the ground temperature. Thus, the magnitude of the urban heat island would decrease if the wind speeds increased.

We proposed to raise building bases away from the ground so that buildings would not block air flows in the surface layer. We performed several numerical simulations by varying the distance between the building base and the ground. If the building base was at the ground the ground temperature downstream of a building was approximately 4 $^{\circ}$C higher than the areas where building effects were free.

If the building base was raised by 10 m above the ground, the ground temperatures in the building areas decreased by 10 $^{\circ}$C. When the building base was raised by 20 m or more, the ground temperatures were almost identical to those without buildings.

The proposed design concept mitigated several adverse effects associated in urban living. For example, higher wind speed was beneficial to decrease air pollution concentration levels. The raised building bases provided shadows and shades to pedestrians.

REFERENCES

Hirt, C.W., and J. L. Cox, 1972: Calculating Three-Dimensional Flows around Structures and over Rough Terrain. J. of Computational Phys., 10, 324-340.

Kao, C.-Y. J. and Yamada, T., 1988: Use of the CAPTEX Data for Evaluation of a Long-Range Transport Numerical Model with a Four-Dimensional Data Assimilation Technique, Monthly Weather Review, 116, pp. 293-206.

Mellor, G. L., and T. Yamada, 1974: A Hierarchy of Turbulence Closure Models for Planetary Boundary Layers. J. of Atmos. Sci., 31, 1791-1806.

Mellor, G. L., and T. Yamada, 1982: Development of a Turbulence Closure Model for Geophysical Fluid Problems. Rev. Geophys. Space Phys., 20, 851-875.

Tominaga, Y., A. Mochida, R. Yoshie, H. Kataoka, T. Nozu, M. Yoshikawa, and T. Shirasawa, 2008: AJI guidelines for practical applications of CFD to pedestrian wind environment around buildings. J. Wind Eng. and Industrial Aerodynamics, 96, 1749-1761.

Yamada, T., 1983: Simulations of Nocturnal Drainage Flows by a q2l Turbulence Closure Model. J. of Atmos. Sci., 40, 91-106.

Yamada, T., 2004: Merging CFD and Atmospheric Modeling Capabilities to Simulate Airflows and Dispersion in Urban Areas. Computational Fluid Dynamics Journal, 13 (2):47, 329-341.

Yamada, T., and S. Bunker, 1988: Development of a Nested Grid, Second Moment Turbulence Closure Model and Application to the 1982 ASCOT Brush Creek Data Simulation. Journal of Applied Meteorology, 27, 562-578.